

## Cross-scale convergence in the carbon balance of managed boreal forests in Northern Sweden

Matthias Peichl<sup>a,\*</sup>, Eduardo Martínez-García<sup>a,b</sup>, Jinshu Chi<sup>a,c</sup>, Natascha Kljun<sup>d</sup>, Anne Klosterhalfen<sup>a,e</sup>, Johannes Larson<sup>a</sup>, Hjalmar Laudon<sup>a</sup>, Tomas Lundmark<sup>a</sup>, Guillaume Monteil<sup>f,g</sup>, Mats B. Nilsson<sup>a</sup>, Anusha Sathyanadh<sup>a,h</sup>, Marko Scholze<sup>f</sup>, Jörgen Wallerman<sup>i</sup>, Peng Zhao<sup>a,j</sup>

<sup>a</sup> Department of Forest Ecology and Management, Swedish University of Agricultural Sciences, SE-901 83 Umeå, Sweden

<sup>b</sup> Natural Resources Institute Finland (Luke), FI-00790, Helsinki, Finland

<sup>c</sup> Earth, Ocean and Atmospheric Sciences Thrust, The Hong Kong University of Science and Technology (Guangzhou), 511453, Guangzhou, China

<sup>d</sup> Centre for Environmental and Climate Science, Lund University, SE-223 62 Lund, Sweden

<sup>e</sup> Bioclimatology, University of Göttingen, 37077 Göttingen, Germany

<sup>f</sup> Department of Physical Geography and Ecosystem Science, Lund University, SE-223 62 Lund, Sweden

<sup>g</sup> Barcelona Supercomputing Center, ES-08034 Barcelona, Spain

<sup>h</sup> Department of Energy and Process Engineering, Norwegian University of Science and Technology (NTNU), NO-7034 Trondheim, Norway

<sup>i</sup> Department of Forest Resource Management, Swedish University of Agricultural Sciences, SE-901 83 Umeå, Sweden

<sup>j</sup> Key Laboratory of Agricultural Soil and Water Engineering in Arid and Semiarid Areas of Ministry of Education, Northwest A&F University, Yangling, Shaanxi 712100, China

### ARTICLE INFO

#### Keywords:

Boreal forest landscape  
Carbon sequestration  
Climate change mitigation  
Forest management  
Scale-dependence  
Spatially-nested monitoring

### ABSTRACT

Boreal forests are globally important carbon (C) sinks, but strategies for maximising their climate benefit remain under debate. Major uncertainties in this discussion arise from contrasting sink-source estimates, which largely emanate from inherent limitations of standard measurement techniques to distinct spatio-temporal scales. Here, we use a spatially-nested measurement framework that integrates bottom-up (forest-plot inventory and chamber-based fluxes) and top-down (eddy-covariance; atmospheric observations and atmospheric transport modelling) approaches to reconcile the C balance of actively managed boreal forests in Northern Sweden across plot-, ecosystem-, landscape-, and regional scales during 2016–2018. We found that 3-year mean estimates of the net ecosystem production (NEP) across plot-, landscape-, and regional scales did not differ significantly, converging into a mean ( $\pm 95\%$  confidence interval) C sink of  $118 \pm 27 \text{ g C m}^{-2} \text{ yr}^{-1}$ . We also noted a convergence across these scales for the 3-means of the NEP components, i.e., gross primary production ( $908 \pm 48 \text{ g C m}^{-2} \text{ yr}^{-1}$ ) and ecosystem respiration ( $790 \pm 40 \text{ g C m}^{-2} \text{ yr}^{-1}$ ). However, estimates of the inter-annual variations in NEP and its components were inconsistent among most scales and measurement approaches. Furthermore, our results indicate a scale-dependency in the NEP response to the 2018 European summer drought, with a greater reduction of NEP observed in bottom-up compared to top-down estimates. Thus, this study consolidates the C sink-strength of managed boreal forests and advocates the need for cross-scale assessments to constrain forest C cycle-climate feedbacks.

### 1. Introduction

Boreal forests contain about one-third-of the global forest carbon (C) pool (Astrup et al., 2018; Pan et al., 2011) and are therefore considered as a key element in policy frameworks for mitigating climate change (European Commission., 2021; Hyyrynen et al., 2023; Lemprière et al.,

2013; Lundmark et al., 2014). Recently, strategies for maximising the climate benefit of boreal forests have been the subject of intense debate, with different actors proposing alternative options ranging from active management to set-aside approaches (Ameray et al., 2021; Bellassen and Luysaert, 2014; Högberg et al., 2021; Petersson et al., 2022; Roebroek et al., 2023). The choice of an optimal strategy is further complicated by

\* Corresponding author.

E-mail address: [matthias.peichl@slu.se](mailto:matthias.peichl@slu.se) (M. Peichl).

<https://doi.org/10.1016/j.agrformet.2025.110926>

Received 30 May 2025; Received in revised form 27 October 2025; Accepted 5 November 2025

Available online 20 November 2025

0168-1923/© 2025 The Authors. Published by Elsevier B.V. This is an open access article under the CC BY license (<http://creativecommons.org/licenses/by/4.0/>).

the fact that changes in climatic conditions are occurring most rapidly in the boreal biome (Gauthier et al., 2015; IPCC, 2021). Thus, a detailed understanding of the boreal forest C cycle and its response to climate feedbacks is necessary to support the development of management strategies that both maximise and sustain the climate benefit of boreal forests in a future climate.

A key uncertainty in this debate is the lack of empirical evidence for consolidating the actual current C sink-source strength of the boreal forest (Bellassen and Luyssaert, 2014), which hampers the development of a reference for evaluating alternative management strategies. Instead, the discussion is convoluted by contrasting findings from individual studies, most of which agree on the C sink function of boreal forests (Artaxo et al., 2022; Bradshaw and Warkentin, 2015), while others challenge this view (Hadden and Grelle, 2016, 2017; Pan et al., 2024), particularly when accounting for disturbance effects (Giles-Hansen and Wei, 2022; O'Sullivan et al., 2024). Even with the absence of natural disturbances, the stand-level C balance of a managed boreal forest may fluctuate within a considerable range, spanning from an annual source of about  $600 \text{ g C m}^{-2} \text{ yr}^{-1}$  to a sink of about  $400 \text{ g C m}^{-2} \text{ yr}^{-1}$  in response to forest structure, fertility, and environmental conditions (Anderson-Teixeira et al., 2018; Luyssaert et al., 2007; Peichl et al., 2023a). Furthermore, our understanding of the sensitivity of the boreal forest C balance to extreme weather events remains incomplete due to the complexity of site- and scale-specific responses (Kljun et al., 2006; Lindroth et al., 2020; Martínez-García et al., 2024; Sippel et al., 2018). Hence, there is a need to reconcile estimates of boreal forest C cycle-climate interactions.

The divergence across empirical studies emanates to a large extent from different approaches used to quantify biosphere-atmosphere exchanges, as standard measurement techniques are inherently limited to distinct spatial scales. Consequently, their estimates are likely to diverge if the sampled space-time continuum exhibits pronounced heterogeneity. Specifically, studies using forest-plot inventory- and chamber-based as well as ecosystem eddy-covariance (EC) flux estimates at the plot (hundreds of  $\text{m}^2$ ) and ecosystem (thousands of  $\text{m}^2$ ) scales, respectively, provide detailed insights into local processes and C budgets (Baldochi et al., 2018; Luyssaert et al., 2007), but their confined spatial extent and dependence on specific local environmental conditions introduce large uncertainties in bottom-up scaling estimates (Desai et al., 2008; Kondo et al., 2020). National forest inventories (NFIs) represent a significant spatial extension of the plot scale approach (Fridman et al., 2014). However, they have an inherent low temporal (i.e., multi-annual) resolution and lack estimates of additional C-cycle components (e.g., litterfall, ground vegetation and fine root production), which limits estimates of the annual ecosystem-scale C balance. Conversely, top-down approaches such as tall-tower EC or atmospheric observations combined with atmospheric transport and dynamic vegetation models (ATM) provide landscape (tens of  $\text{km}^2$ ) to regional (hundred thousands of  $\text{km}^2$ ) C budgets, respectively, but lack details on local sinks and sources as well as on underlying mechanistic drivers (Chi et al., 2019; Foster et al., 2023; Kondo et al., 2020). In addition, the ATM approach relies primarily on models that cannot be empirically validated at such large scales (Kondo et al., 2020; Lauvaux et al., 2009). Measurement approaches also differ in their temporal resolution, capturing processes from half-hourly (i.e., EC) to annual (i.e., forest-plot inventory) scales (Campioli et al., 2016). Furthermore, they differ conceptually by estimating C balances via monitoring of either fluxes (i.e., chamber- and EC-based methods), concentrations (i.e., ATM), or stock changes (i.e., forest-plot inventory), each associated with specific sources of measurement error (Peichl et al., 2010; Sathyanadh et al., 2021). Therefore, achieving agreement among these approaches requires sufficiently homogeneous conditions in both space and time. In practice, however, this prerequisite is rarely met, and related uncertainties are greatly increasing in spatially heterogeneous landscapes subject to active management (Desai et al., 2022a; Peichl et al., 2023a; Zhu et al., 2023).

To reduce the uncertainty arising from scale-dependency, nested

monitoring programmes bridging these various spatio-temporal scales are required (Bastviken et al., 2022; Futter et al., 2023). However, given the extensive need for resources, such integrated measurement frameworks are scarce to date. Consequently, the extrapolation of local empirical information across the heterogeneous time-space continuum commonly relies on simulations from process-based ecosystem models (Piao et al., 2013) and machine-learning methods (Zeng et al., 2020). However, the limited availability of integrated measurement frameworks severely hampers the empirical validation of such extrapolation efforts.

To overcome these limitations, we provide here for the first time an integrated analysis of empirical C balance estimates from a unique spatially-nested measurement network spanning from plot- to regional scale across a managed landscape dominated by coniferous forests in northern Sweden (Fig. 1). Specifically, our cross-scale assessment combined flux data from the 1) *plot* scale, based on forest-plot inventory and chamber-based measurements across 57 forest stands of various ages (5 to 211 years old); 2) *ecosystem* scale, measured by conventional EC; 3) *landscape* scale, obtained from bottom-up scaling of forest-plot scale data (L-Plot) and tall-tower EC data (L-EC, as top-down approach); and 4) *region* scale (i.e., Swedish Norrland region), based on bottom-up scaling of forest-plot scale data from the Swedish National Forest and Soil Inventories (NFI) and via the ATM top-down approach. Our main objectives were i) to reconcile the net ecosystem production (NEP; i.e., the C sink-source strength based on land-atmosphere  $\text{CO}_2$  exchanges) across these four different scales during 2016–2018 and ii) to compare scale-specific NEP responses to the exceptional 2018 European summer drought.

## 2. Methods

### 2.1. Study area

The centre of our spatially-nested monitoring framework was located in the Krycklan Catchment Study (KCS) area in northern Sweden ( $64^\circ 14' \text{N}$ ,  $19^\circ 46' \text{E}$ ; Fig. 1, Supplementary Fig. S1), which encompasses  $68 \text{ km}^2$  of a typical boreal managed forest landscape in this region (Laudon et al., 2021). The climate is cold temperate humid with a 30-year (1991–2020) mean annual precipitation of  $638 \pm 40 \text{ mm}$  and a mean annual air temperature of  $2.4 \pm 0.3 \text{ }^\circ\text{C}$ . The landscape is dominated by a mosaic of forests (87.5 %) with contributions from mires (7.6 %), artificial areas (2.0 %), agricultural lands (1.9 %), and inland waters (i.e., lakes and streams, 1.0 %). The forest stands include predominantly Scots pine (*Pinus sylvestris* L., 63 %) and Norway spruce (*Picea abies* (L.) H. Karst., 26 %) mixed with deciduous trees (*Betula* spp., *Alnus incana* (L.) Moench., and *Populus tremula* L., 11 %). Most of the forested area is managed by conventional rotation-forestry, including predominantly even-aged stands, which are mostly artificially regenerated. The wider study region spanned the Swedish Norrland region, which experiences a boreal climate (Köppen code: Dfc), although with pronounced north-south and east-west gradients in annual mean air temperature, as well as local variations in precipitation. A comparison of tree growth records from KCS and NFI data for the Norrland region suggests that growth rates in KCS are within the lower and upper limits defined by the northern and southern Norrland sub-regions, respectively (Supplementary Fig. S2).

### 2.2. Plot-scale C balance estimates based on forest-plot inventory and chamber-based flux measurements

We initially selected 50 main forest plots within stands ranging in age from 5 to 211 years after stand establishment from a regular grid ( $350 \text{ m} \times 350 \text{ m}$ ) of 436 permanent forest inventory plots spanning the KCS (Martínez-García et al., 2022). This dataset was later expanded with 7 additional forest plots located in old stands as described in Peichl et al. (2023a). For each of the 57 forest plots, we determined the annual net

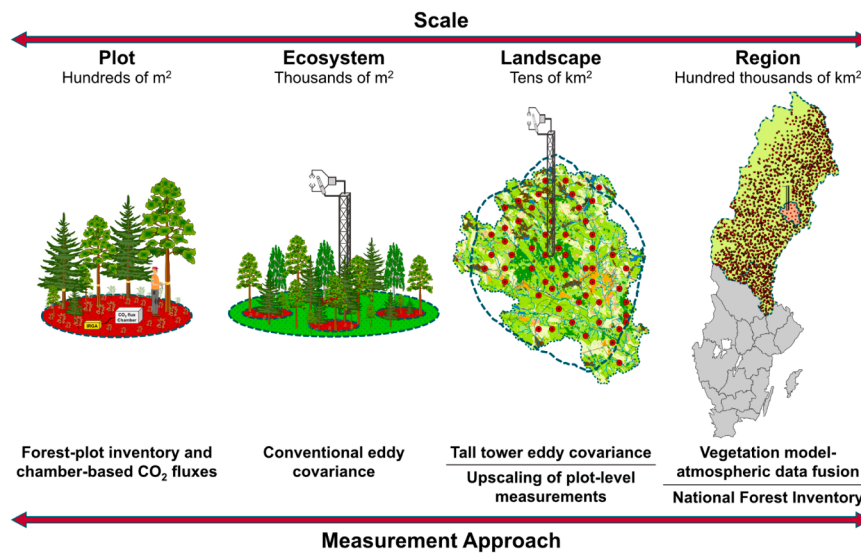


**Fig. 1.** Schematic illustration of the spatially-nested flux measurement framework that integrates approaches to measure the forest carbon balance at plot, ecosystem, and landscape scales within the Krycklan catchment, and at the region scale for Northern Sweden. Note that the plot size, ecosystem boundary, and landscape contour within the region are not to scale and for illustrative purposes only.

ecosystem production (NEP) during 2016–2018 from the balance between total net primary production (NPP) and total heterotrophic respiration ( $R_h$ ) based on a combination of forest-plot inventory- and chamber-based soil  $CO_2$  flux measurements as described in detail by Martínez-García et al. (2022) and Peichl et al. (2023a). Briefly, annual NPP was estimated as the sum of above- and belowground NPP of trees and understory vegetation ( $NPP_t$  and  $NPP_u$ , respectively), whereas annual  $R_h$  included heterotrophic respiration fluxes from soil and dead wood ( $R_{hs}$  and  $R_{hdw}$ , respectively). Specifically,  $NPP_t$  for the 50 main forest plots was determined based on annual changes in tree above- and belowground (coarse root) biomass and detritus production. Annual tree biomass was estimated from annual inventories of tree diameter (at breast height) and height data, which served as input for established allometric biomass equations (Marklund, 1988; Petersson and Ståhl, 2006; Repola, 2008). Annual detritus production was collected with litter traps. Aboveground  $NPP_u$  was determined through destructive sampling, while both belowground fine root production of trees and understory vegetation were quantified using the ingrowth core method, following the methodology detailed by Martínez-García et al. (2022). In these 50 main forest plots,  $R_{hs}$  was determined every 3–4 weeks based on chamber measurements conducted in experimental vegetation removal/trenching plots, which were extrapolated to the annual scale based on empirical relationships with soil temperature (Martínez-García et al., 2022).  $R_{hdw}$  was derived by applying decay functions to the deadwood stock. For the 7 additional forest plots, annual tree biomasses were estimated using the same approach as for the 50 main forest plots. The remaining NPP and  $R_h$  components were derived from fixed ratios and/or functional relationships based on stand basal area established from the 50 main forest plots. These methods are described in detail in Peichl et al. (2023a) and summarized in the Supplementary materials, Section 1.

To estimate the gross primary production of trees ( $GPP_t$ ) for the 57 forest plots, we multiplied  $NPP_t$  by the carbon use efficiency of boreal trees ( $CUE_t$ ), with the latter estimated using data from Tang et al. (2014). Gross primary production of understory vegetation ( $GPP_u$ ) was estimated with the chamber technique at the 50 main forest plots following Martínez-García et al. (2022). For the 7 additional forest plots, we applied a stand age-based functional relationship derived from the 50 main forest plots to estimate the annual carbon use efficiency of understory vegetation ( $CUE_u$ ). We then used the ratio  $NPP_u:CUE_u$  to

estimate  $GPP_u$  in these 7 forest plots. Further details on the methodologies used to estimate  $GPP_t$  and  $GPP_u$  are provided in Supplementary materials, Section 2. Annual GPP for all 57 forest plots was then calculated as the sum of  $GPP_t$  and  $GPP_u$ , while their annual ecosystem respiration (Reco) was derived as the difference between GPP and NEP.

### 2.3. Ecosystem-scale C balance estimates from conventional eddy covariance measurements

We compiled eddy-covariance (EC) based estimates of annual NEP and its underlying GPP and Reco component fluxes during 2016–2018 for two mature boreal forest stands at the Rosinedal flux station (SE-Ros; in this study referred to as 'EC-Ros' to indicate that measurement method and scale are based on the EC technique) and at the Integrated Carbon Observation System (ICOS) Svartberget ecosystem station (SE-Svb; in this study hereafter referred to as 'EC-Svb'). The EC-Ros station ( $64^{\circ}10'N$ ,  $19^{\circ}45'E$ , 145 m a.s.l.) is a ~100-year-old pine stand growing on sandy soil located about 10 km south of the KCS. The EC-Svb station ( $64^{\circ}15'N$ ,  $19^{\circ}46'E$ , 257 m a.s.l.) is a ~110 year-old mixed stand of spruce (61 %), pine (34 %), and birch (5 %) located close to the centre of the KCS. Flux data for EC-Ros were obtained from Zhao et al. (2022), whereas the flux data for EC-Svb were acquired from the database of the ICOS warm winter initiative database (<https://www.icos-cp.eu/data-products/2G60-ZHAK>). Post-processing, NEP gap-filling, and flux-partitioning of EC-based NEP data into GPP and ER estimates (based on the night-time approach) were performed according to ICOS protocols (Franz et al., 2018). It should be noted that no flux data were available at the EC-Svb station for 2017. A detailed description of the forest site characteristics and the EC measurement setups for both EC-Ros and EC-Svb is provided in previous studies (Chi et al., 2019, 2020, 2021; Zhao et al., 2022). A summary of the setup and data processing is also included in Supplementary materials, Section 3. It is noteworthy that, in contrast to the other studied scales which integrated information from a wide range of stand developmental stages (i.e., recent clear-cuts to >200-year-old stands), our ecosystem-scale C balance estimates from conventional EC measurements provide only a snapshot estimate for stands in the mature development phase. Consequently, this scale was excluded from the analysis of the convergence of annual C budgets across various scales.

#### 2.4. Landscape-scale C balance estimates from tall tower EC measurements and bottom-up scaling of plot-scale data

The ICOS Svartberget combined atmospheric-ecosystem station includes a 150 m tall tower along which an additional EC system was deployed in 2016 at 70 m height to conduct tall tower EC measurements (L-EC). Annual NEP, GPP, and Reco estimates were obtained from this setup during 2016–2018. The flux footprint of these L-EC measurements was derived using the FFP footprint model (Kljun et al., 2015) and has a radius of several km and spans roughly over the KCS area. We note that the L-EC flux-footprint integrates not only forest stands, but also mires, artificial areas, agricultural lands, and inland waters. However, given that forest cover contributes around 80 % to the footprint area, we assume that the annual flux estimates primarily account for this land cover. Details on the L-EC set up, data post-processing including NEP gap-filling and partitioning into GPP and ER, and results have been previously described (Chi et al., 2019, 2020; Klosterhalfen et al., 2023) and are summarized in the Supplementary materials, Section 4.

As an alternative landscape-scale approach, we developed a bottom-up estimate (L-Plot) of annual NEP, GPP, and Reco during 2016–2018 based on scaling the plot-scale data to the forested areas of the KCS. It is noteworthy that the 57 selected forest plots originally did not include information on the C emission fluxes occurring during the first 4 years after harvest (Peichl et al., 2023b). To address this shortcoming, we extended our dataset with EC-based NEP, GPP, and Reco estimates from recent boreal clear-cuts (Supplementary Fig. S3). The IAV of these C fluxes was calculated from the annual C fluxes of the 3 recent clear-cuts (5–7 years-old) included in the selected forest plots. We further note that the difference in the convergence estimate based on the original 57 plots and the extended dataset was minor (Supplementary Fig. S4). Using this extended dataset, we first derived empirical functions to estimate plot-level stand age based on tree biomass (Eq. (1)). We then developed additional empirical functions to estimate plot-level annual NEP and GPP for each the 3-year study period, using stand age (accounting for its annual increase) as predictive variable (Eqs. (2) and 3, respectively).

$$\text{Age} = (b_0 + b_1 \times \text{sqrt}(\text{Biomass}))^2 \quad (1)$$

$$\text{NEP} = b_0 + b_1 \times \ln(\text{Age}) + b_2 \times \ln(\text{Age})^2 \quad (2)$$

$$\text{GPP} = \exp(b_0 + b_1 \times \ln(\text{Age}) + b_2 \times \ln(\text{Age})^2) \quad (3)$$

We subsequently scaled NEP and GPP across the forested areas of the KCS using a high-resolution Lidar-based biomass raster map, resampled to 1 m × 1 m resolution from an original 12.5 m × 12.5 m grid. This raster served as the basis for estimating stand age at each biomass pixel using Eq. (1), followed by the calculation of NEP and GPP for each age pixel using Eqs. (2) and 3, respectively. Finally, annual Reco was calculated for each pixel by subtracting NEP from GPP across the forested areas. See Supplementary materials, Section 5, for further details of this L-Plot approach.

#### 2.5. Region-scale C balance estimates from atmospheric observations combined with vegetation models and bottom-up approach based on plot-scale NFI data

For the ATM approach, we compiled regional-scale estimates of the annual NEP, GPP, and Reco for the Norrland region in Sweden during 2016–2018 from three dynamic vegetation models, including LPJ-GUESS (Smith et al., 2014), ORCHIDEE (Krinner et al., 2005), and VPRM (Mahadevan et al., 2008). These model estimates were then constrained using atmospheric observations of CO<sub>2</sub> concentrations at the ICOS Svartberget atmosphere station and five additional ICOS atmosphere stations in Fennoscandia, in combination with the Lund

University Modular Inversion Algorithm (LUMIA) transport model (Monteil and Scholze, 2021). The latter relies on the FLEXPART 10.4 Lagrangian transport model (Pisso et al., 2019), for computing the regional transport of the fluxes in a domain ranging from 0°W, 54°N to 20°E, 70°N, and uses prescribed background concentrations from a global TM5 inversion. LUMIA then computes the CO<sub>2</sub> concentrations at the atmosphere stations in the domain using the model estimates of the surface CO<sub>2</sub> fluxes (NEE and anthropogenic emissions), gridded on a 0.5° × 0.5° and 3-hourly resolution. The details of this ATM approach used to estimate the region-scale C balance were described by Sathyanadh et al. (2021), with a summary provided in Supplementary materials, Section 6.

An alternative regional-scale estimate (i.e., NFI approach) of NEP, GPP and Reco was derived by scaling plot-level data from the Swedish National Forest and Soil Inventories to the Norrland region in Sweden during 2016–2018. In this NFI approach, we first extracted the annual increment of stem volume for 20-year stand age classes (i.e., 0–20, 21–40, ... > 121 years) across Norrland from the National Forest Inventory database, which was then converted into the annual increment of whole tree biomass via biomass expansion factors. Using data from the 50 main forest plots, we then developed empirical functions to derive the annual estimates for the remaining NPP components (i.e., litterfall and NPP<sub>u</sub>) based on stand age for each age class. Next, we defined empirical functions between the soil organic carbon (SOC) turnover ( $\tau_s$ ), which is the ratio of SOC in the organic and upper mineral soil layers up to 0.2 m depth to annual Rh<sub>s</sub>, and stand age, using data from the 50 main forest plots. Additionally, we extracted the SOC for the organic and upper mineral soil layers (10 cm intervals) up to 0.5 m depth across Norrland extracted from the National Forest Soil Inventory database. These SOC estimates were then extrapolated to a depth of 1 m using the relationship between SOC and soil depth derived from the 6 sampled upper soil layers. By applying the ratio of SOC from the soil inventory (1 m) to that obtained on the plots (0.2 m), and incorporating  $\tau_s$ , we estimated  $\tau_s$  up to 1 m depth. This was done to validate our  $\tau_s$  estimates against those reported for boreal forests in previous studies (Carvalhais et al., 2014). Finally, annual Rh<sub>s</sub> for each stand age class was computed by dividing the SOC up to 1 m depth across Norrland by the annual  $\tau_s$  up to 1 m depth during 2016–2018. In addition, the annual hard and decomposed dead wood pools extracted from the National Forest Inventory database for each stand age class were multiplied by species- and decay class-specific decomposition rate constants (Shorohova et al., 2008; Yatskov et al., 2003) to calculate the annual Rh<sub>dw</sub>. Annual NEP for the Norrland region was then calculated based on the balance between the measured and modelled components of NPP and Rh. Subsequently, regional GPP<sub>t</sub> and GPP<sub>u</sub> were calculated by dividing the regional NPP<sub>t</sub> and NPP<sub>u</sub> estimates by their respective CUE<sub>t</sub> and CUE<sub>u</sub>, with the latter defined in the plot-scale approach (see Section 2.2). Finally, the annual Reco for the region was computed as the balance of regional GPP<sub>t</sub> + GPP<sub>u</sub> – NEP estimates. A detailed description of this NFI approach for estimating the region-scale C balance is provided in Supplementary materials, Section 7.

#### 2.6. Drought anomalies in annual NEP

In the summer of 2018, a record-breaking, hot drought occurred across large areas of central and northern Europe (Peters et al., 2020). For comparison, the year 2016 experienced average air temperature and precipitation patterns relative to the period 1991–2020 and was therefore considered as a normal climatic year (Supplementary Fig. S5). The impact of the 2018 drought event in the annual NEP of each of the investigated scales was evaluated by estimating the absolute anomaly (g C m<sup>-2</sup> yr<sup>-1</sup>,  $\Delta\text{NEP}$ ) between the reference year 2016 and 2018 according to Eq. (4).

$$\Delta\text{NEP} = \text{NEP}_{2018} - \text{NEP}_{2016} \quad (4)$$

## 2.7. Statistics

The non-parametric Kruskal–Wallis rank sum test followed by a Dunn–Bonferroni post hoc test ( $p \leq 0.05$ ) was performed to test for significant differences in the 3-year means of annual NEP, GPP, Reco, and  $\Delta\text{NEP}$  among the plot-, landscape-, and region scales. The cross-scale mean and range ( $\pm 95\%$  confidence interval) for each NEP, GPP, Reco, and  $\Delta\text{NEP}$  were estimated from the 3-year mean values of the plot-, landscape-, and region scales. The ecosystem scale was excluded in these cross-scale estimates since data were only available for mature stands at this scale. Furthermore, we note that the estimates derived from the L-Plot and NFI approaches are not fully independent from the plot-scale estimate. This dependency arises from the use of data from the 50 main forest plots in the development of the empirical functions relating C fluxes to stand age, which were then used for scaling NEP to the landscape (L-Plot approach) and region scale (NFI approach). Spatial analyses were conducted using the ArcGIS software (version 10.5; ESRI, Redlands, CA, USA), while statistical analyses were conducted using the SPSS software (version 29.0; IBM corp., Armonk, NY, USA).

## 3. Results

### 3.1. Cross-scale comparison of forest age structure

Given the strong influence of stand age on NEP, we first evaluated the stand age distribution across the various study scales to assess the homogeneity across the space-time continuum. Mean stand age for the plot, landscape and region scales ranged between 69 and 87 years, without significant differences among these scales (Fig. 2). The mean age of the mature stands at the ecosystem scale (105 years) was not

significantly different from that of the mature stands in the plot-level dataset (98 years). Furthermore, the age class distributions were comparable at the landscape- and region-scales, with both showing a tendency towards greater contribution from younger age classes (0–60 years) (Fig. 2). In contrast, at the plot scale, there was a peak in the 61–80 year age class. In addition, the younger age classes (0–60 years) contributed less at this plot scale (about 5 to 13 %) compared to the landscape and region scales, whereas an opposite bias (about 3 to 18 %) was consequently present in the older age classes (> 61 years).

### 3.2. Cross-scale convergence in the C sink-strength of managed boreal forests

Our results show that at the lowest spatial scale, i.e., the plot-scale, annual NEP estimates ranged from  $-131$  to  $+406 \text{ g C m}^{-2} \text{ yr}^{-1}$ , indicating a manifold variation including both sinks and sources across diverse forest stands for the managed boreal forest landscape in northern Sweden (Fig. 3a). Notably, however, our empirical cross-scale assessment revealed that the 3-year mean NEP of the plot-, landscape-, and region scales were not significantly different, converging to a mean C sink estimate of  $118 \pm 27 \text{ g C m}^{-2} \text{ yr}^{-1}$  (mean  $\pm 95\%$  confidence interval) (Fig. 3). It is important to note that this convergence estimate did not include the ecosystem scale, as the two mature forest stands measured by EC (Fig. 3b) represent only a selective sample during stand development. However, further analysis showed that these ecosystem-scale NEP estimates were within the range of their respective plot-scale estimates in mature (90–120 year-old) forest stands (Supplementary Fig. S6).

In contrast to the convergence of the 3-year mean NEP, estimates of the inter-annual variations (IAV) of NEP were inconsistent across the various scales and measurement approaches (Fig. 3). Specifically, the IAV of NEP agreed well among the plot, landscape bottom-up (L-Plot),

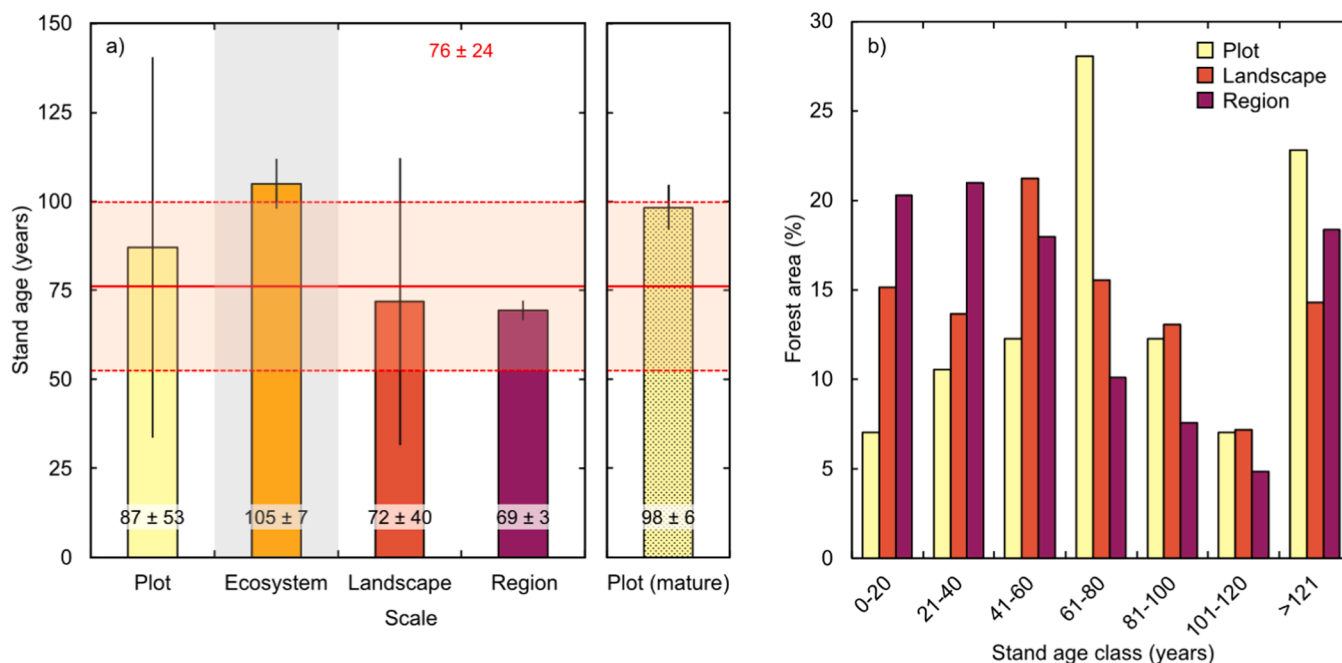


**Fig. 2.** Comparison of the forest stand age among the plot, ecosystem, landscape, and region scales. a) Mean stand age for each scale. Mature forest plots (90–120 years old;  $n = 8$ ) for the ‘Plot’ scale are also shown. The values for the ‘Ecosystem’ scale were obtained from the mature forests Rosinedal and Svartberget, which were classified within the 101–120 stand age class. Values and error bars represent the means and standard deviations, respectively. The value highlighted in red shows the convergence stand age (mean  $\pm 95\%$  confidence interval) estimated from the means of the plot, landscape, and region scales. The bar for the ‘Ecosystem’ scale is shaded to indicate that this value was excluded in the estimation of the convergence stand age. b) Distribution of stand age classes (%) relative to the total forest area. The values for the ‘Plot’, ‘Landscape’ and ‘Region’ scales in both panels a) and b) were based on 57, 476, and 1341 plots, respectively. Note that the plots used for the ‘Region’ scale were obtained from the Swedish National Forest Soil Inventory.

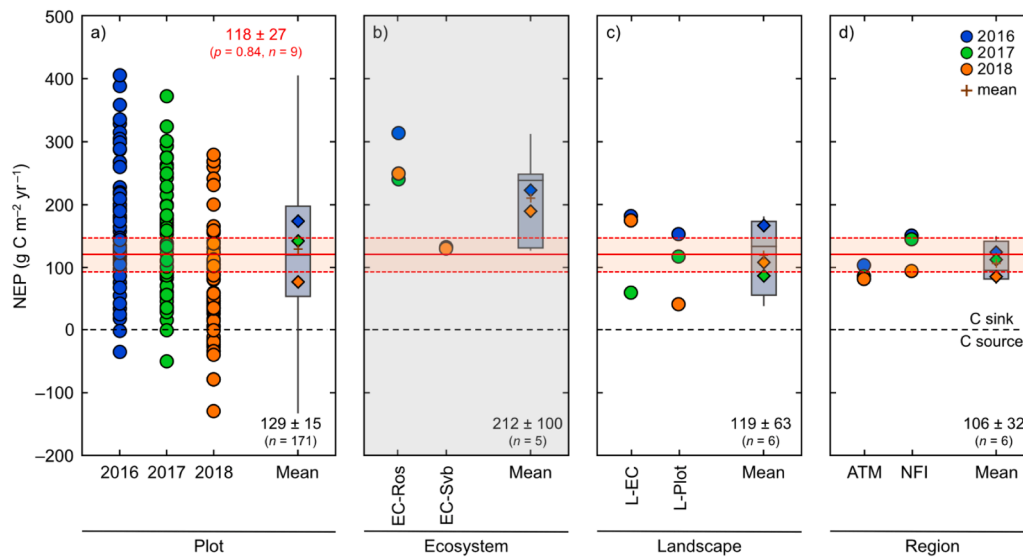


**Fig. 3.** Convergence of the net ecosystem production across the plot, ecosystem, landscape, and region scales. The panels a)–d) show the annual net ecosystem production (NEP,  $\text{g C m}^{-2} \text{ yr}^{-1}$ ) for a boreal forest in Sweden for the different approaches used at the plot, ecosystem, landscape, and region scales, respectively, during 2016–2018. Plot scale data are based on forest-plot inventory and chamber-based measurements of carbon dioxide ( $\text{CO}_2$ ) fluxes carried out in 50 main and 7 additional old forest (‘Plots’), in stands ranging in age from 5 to 211 years. Ecosystem scale data are based on conventional eddy covariance (EC) measurements carried out at the EC stations Rosinedal (‘EC-Ros’;  $\sim 100$ -year old homogenous Scots pine stand) and Svartberget (‘EC-Svb’;  $\sim 103$ -year-old mixed spruce-pine stand, data available for 2016 and 2018). Landscape scale data are based on: 1) tall tower EC measurements (‘L-EC’) carried out at 70 m height on the ICOS-Svartberget combined atmospheric-ecosystem station, and 2) the bottom-up scaling of  $\text{CO}_2$  fluxes from plot to landscape scale (‘L-Plot’). Region scale data are based on: 1) fusion of vegetation models and atmospheric concentration data (‘ATM’), and 2) plot-level  $\text{CO}_2$  flux estimates based on data from the plot scale and the Swedish National Forest and Soil Inventories (‘NFI’). Circular closed symbols indicate annual NEP values for each approach. Box plots present the mean annual NEP values for each scale (diamond symbols), with boxes representing the 25th (bottom) and 75th (top) percentiles, the central line and cross showing the median and mean, respectively. Whiskers above and below the boxes denote data within 1.5 times of the interquartile range. Values below each box plot indicate the mean  $\pm 95\%$  confidence interval. The  $p$ -value for the non-parametric Kruskal–Wallis rank sum test comparing the differences between the annual NEP means of plot, landscape, and region scales is also shown. The value in red font shows the NEP convergence mean  $\pm 95\%$  confidence interval (calculated from the plot, landscape, and region scale data), with the latter two visualized by the horizontal red straight and dashed lines, respectively. Panel b) is shaded to indicate that these values were excluded in the estimate of NEP convergence. The horizontal dashed black line indicates the carbon (C) source-to-sink transition.

and regional (ATM and NFI) estimates suggesting the highest and lowest NEP in 2016 and 2018, respectively. In comparison, the IAV differed in the landscape EC (L-EC) estimate, which suggested the lowest NEP during 2017.

Further analysis showed that cross-scale convergence also occurred for both underlying NEP component fluxes, i.e. gross primary production (GPP) and ecosystem respiration (Reco). Specifically, GPP and Reco at the plot, landscape- and region-scale were not significantly different, converging to 3-year mean estimates of  $908 \pm 48$  and  $790 \pm 40$   $\text{g C m}^{-2} \text{ yr}^{-1}$ , respectively (Fig. 4). However, we also observed inconsistent IAV patterns for GPP and Reco across scales and between alternative approaches at a given scale (Supplementary Figs. S7 and S8). At the regional scale, it is notable that the estimates from ATM and NFI approaches suggested different IAV for GPP (and differences in the magnitude for Reco), despite the agreement on the IAV of NEP between both approaches.

### 3.3. Scale-dependent response of the boreal forest C balance to drought

As our data from all scales and measurement approaches comprised the exceptional European summer drought in 2018, we were further able to compare the drought-response of NEP from plot to regional scales. We found that relative to the normal climatic year 2016, annual NEP decreased in response to drought at all scales in 2018, with a mean reduction of  $-65 \pm 70$   $\text{g C m}^{-2} \text{ yr}^{-1}$  (Fig. 5). However, the reduction in NEP at the plot-scale ( $-95 \pm 15$   $\text{g C m}^{-2} \text{ yr}^{-1}$ ) was two-fold larger than at larger scales, at which the NEP reduction was within a narrow range of  $33$ – $59$   $\text{g C m}^{-2} \text{ yr}^{-1}$ . At the plot-scale, the estimates ranged widely from

small positive ( $+20$   $\text{g C m}^{-2} \text{ yr}^{-1}$ ) to large negative ( $-224$   $\text{g C m}^{-2} \text{ yr}^{-1}$ ) drought responses (Fig. 5a). At the ecosystem scale, we observed a considerable difference in the drought responses estimated by EC between the two contrasting mature forest stands, suggesting a negligible response at the mixed pine-spruce forest EC-Svb compared to NEP reduction of  $65$   $\text{g C m}^{-2} \text{ yr}^{-1}$  at the pine stand EC-Ros (Fig. 5b). Furthermore, the comparison of alternative measurement approaches at the landscape and regional scales suggests a larger reduction in NEP due to drought in the plot-based bottom-up estimates (i.e., L-Plot, NFI) compared to the top-down estimates (i.e., L-EC, ATM) (Fig. 5c and d).

## 4. Discussion

### 4.1. Reconciling the C balance of managed boreal forests across different spatial scales

The results from our cross-scale assessment provide valuable empirical evidence that consolidates the magnitude of the C sink-strength of actively managed boreal forests in northern Sweden. Our findings highlight that despite the presence of both local sinks and sources (i.e., recently harvested stands) of C within the managed forest landscape, these converge to a significant C sink when aggregated over spatial and temporal scales that account for both the full stand rotation period and inter-annual variations in weather conditions. The observed cross-scale convergence may thus serve as a benchmark for future evaluations of the C balance and associated climate impacts of alternative forest management strategies for boreal forests. It is noteworthy that our estimated mean C sink of  $118 \pm 27$   $\text{g C m}^{-2} \text{ yr}^{-1}$  for this actively

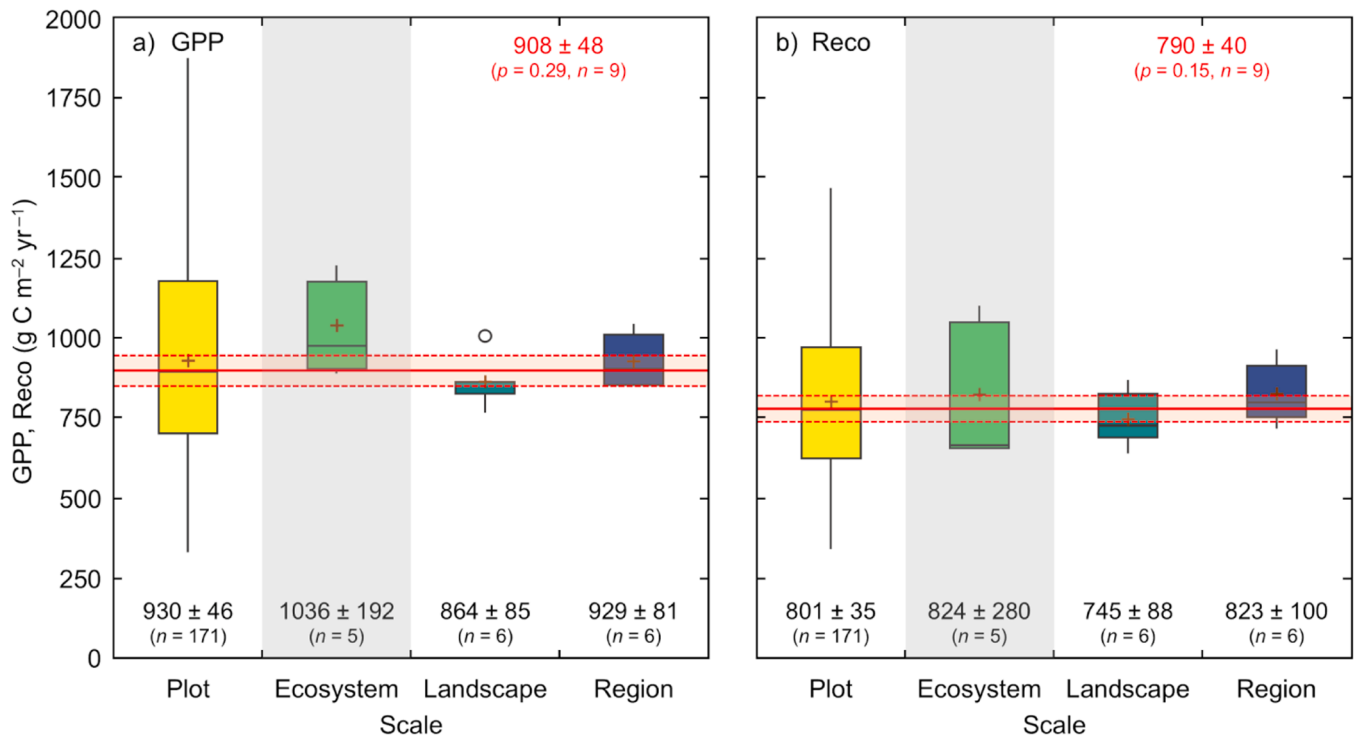


**Fig. 4.** Convergence of gross primary production and ecosystem respiration across the plot, ecosystem, landscape, and region scales. The panels a) and b) show the mean annual gross primary production (GPP,  $\text{g C m}^{-2} \text{ yr}^{-1}$ ) and ecosystem respiration (Reco,  $\text{g C m}^{-2} \text{ yr}^{-1}$ ) for the plot, ecosystem, landscape, and region scales, respectively, during 2016–2018. The boxes represent the 25th (bottom) and 75th (top) percentiles, the central line and cross the median and mean, respectively. Whiskers above and below the boxes denote data within 1.5 times of the interquartile range and outliers are given as individual circular points. Values below each box-plot indicate the mean  $\pm$  95 % confidence interval. The  $p$ -values for the non-parametric Kruskal–Wallis rank sum test comparing the differences between the annual GPP and Reco means of plot, landscape, and region scales are also shown. The value in red font shows the GPP and Reco convergence means  $\pm$  95 % confidence intervals (calculated from the plot, landscape, and region scale data), with the latter two visualized by the horizontal red straight and dashed lines, respectively. Box-plots of the ecosystem scale are shaded to indicate that these values were excluded in the estimation of GPP and Reco convergences.

managed forest landscape in northern Sweden is about three times higher than the average value reported for all boreal forests globally ( $38.5 \pm 4.4 \text{ g C m}^{-2} \text{ yr}^{-1}$ ; Pan et al., 2024), suggesting a stronger C sink in managed compared to unmanaged boreal forests. Furthermore, our C sink estimate exceeds by more than twice that of the mean emission removal rate for forest land ( $44 \text{ g C m}^{-2} \text{ yr}^{-1}$  averaged over 2016–2018) reported in Sweden’s national LULUCF accounting to the IPCC (UNFCCC, 2023a, b; M. Lundblad, pers. comm.). This divergence may partially reflect the contributions from greatly reduced NEP in central and southern Swedish forests during the 2018 drought year (Lindroth et al., 2020) in the national accounting, relative to our northern study domain, besides methodological differences between both measurement approaches. Overall, given the large spatio-temporal variations in the boreal forest C sink-source strength, our findings strongly advocate caution when extrapolating C balance estimates (e.g., from single-site studies) beyond their distinct spatial and temporal boundaries and emphasize the need for cross-scale validation to constrain forest C budgets.

The observed convergence of 3-year averages of GPP and Reco across plot, landscape- and region-scales is further noteworthy, considering the conceptual differences among the various approaches used to estimate these NEP component fluxes. Specifically, plot-scale assessments based on forest-plot inventory data combined with chamber-based flux measurements aggregate GPP and Reco from estimating multiple contributing fluxes across the tree canopy-forest floor-soil continuum, each of which introduces inherent uncertainty (Carnieli et al., 2016; Peichl et al., 2010). In contrast, EC-based approaches rely on simple semi-empirical models to partition the measured net  $\text{CO}_2$  exchange into

GPP and Reco (Reichstein et al., 2005). While GPP and Reco estimates from biometric- and EC-based methods have previously shown reasonable agreements for forest ecosystems globally, a bias towards lower biometric GPP estimates was noted particularly for the boreal region (Carnieli et al., 2016). In contrast, mismatches in Reco explained inconsistencies in NEP estimates from multiple EC and tall-tower flux measurements over a heterogeneous forest landscape in northern Wisconsin (Desai et al., 2022a). Possible causes for divergence between local and regional-scale estimates could be disturbances (e.g., windthrows, fires and/or insect outbreaks) as well as contributions from non-forest ecosystems (e.g., mires and lakes) not captured by plot and ecosystem-scale approaches. This finding suggests that the observed cross-scale convergence in actively managed boreal forests in northern Sweden was likely facilitated by the absence of natural disturbances, in contrast to less intensively managed boreal regions in Canada and Russia which are especially prone to additional emissions due to wildfires (Giles-Hansen and Wei, 2022; Högberg et al., 2021; Virkkala et al., 2025). In addition, the multi-year flux convergence observed in our study was likely supported by the relatively uniform stand age distribution across scales (Fig. 2) and the comparable forest productivity observed between the selected landscape and regional domains (Supplementary Fig. S2).

Predicting and resolving contrasting patterns of the inter-annual variability (IAV) in terrestrial C fluxes remains a key challenge in both empirical and modelling studies (Desai et al., 2010; Keenan et al., 2012). Similarly, we observed considerable discrepancies in the IAV of NEP among scales and measurement approaches, despite the observed cross-scale convergence in the 3-year mean NEP. This suggests that the

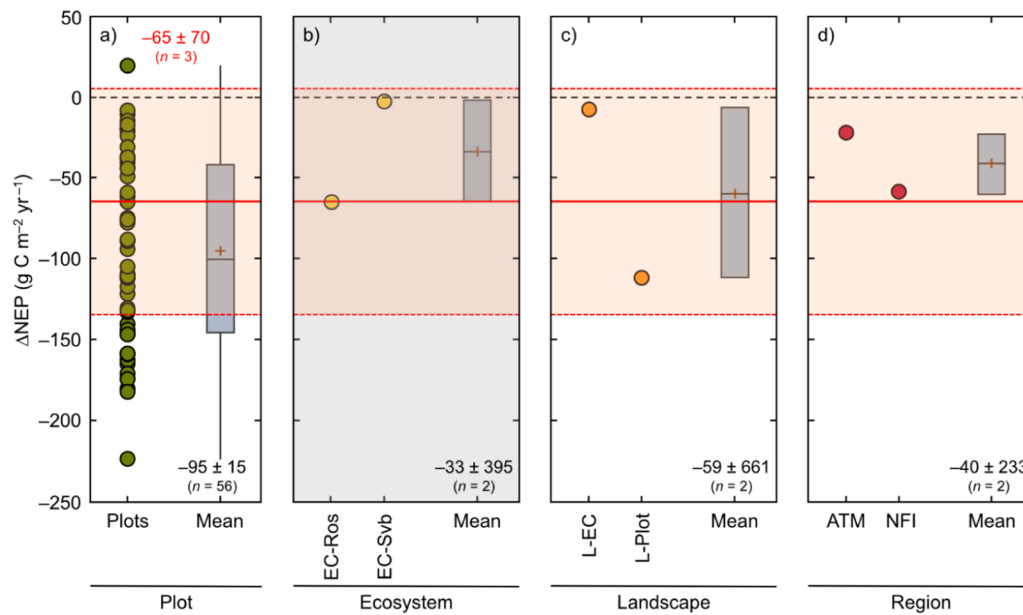


**Fig. 5.** Absolute drought anomaly of net ecosystem production across the plot, ecosystem, landscape, and region scales. The absolute anomaly of the net ecosystem production ( $\Delta\text{NEP}$ ,  $\text{g C m}^{-2} \text{ yr}^{-1}$ ) of the drought year 2018 calculated relative to the reference year 2016 ( $\Delta\text{NEP} = \text{NEP}_{2018} - \text{NEP}_{2016}$ ) for the plot, ecosystem, landscape, and region scales, respectively. A description of the ‘Plots’, ‘EC-Ros’, ‘EC Svb’, ‘L-EC’, ‘L-Plot’, ‘ATM’, and ‘NFI’ approaches is provided in Fig. 1 in the main text. The boxes represent the 25th (bottom) and 75th (top) percentiles, the central line and cross the median and mean, respectively. Whiskers above and below the boxes denote data within 1.5 times of the interquartile range. Values below each box-plot indicate the mean  $\pm$  95 % confidence interval. The value in red font shows the  $\Delta\text{NEP}$  convergence mean  $\pm$  95 % confidence interval (calculated from the plot, landscape, and region scale data), with the latter two visualized by the horizontal red straight and dashed lines, respectively. Box-plot of the ecosystem scale is shaded to indicate that these values were excluded in the estimation of  $\Delta\text{NEP}$  convergence. Horizontal dashed black line indicates the negative-to-positive transition of the absolute drought anomaly. A non-parametric Kruskal–Wallis rank sum test shows no significant differences ( $p = 0.18$ ) when comparing the differences between the mean  $\Delta\text{NEP}$  values of the plot, landscape, and region scales.

dominant processes (e.g., stem diameter growth, turbulent biosphere-atmosphere exchanges and atmospheric dispersion, etc.) captured by the various measurement approaches have different sensitivities to the various environmental drivers of IAV, which may include multi-factorial effects from weather, phenology and hydrology (Desai et al., 2010). Furthermore, temporal lags and carry-over effects in the allocation of assimilated C to woody biomass may cause divergence between biometric- and EC-based NEP estimates (Cabon et al., 2022; Campioli et al., 2016; Peichl et al., 2010). Thus, process-specific responses to environmental drivers may explain scale-dependency, resulting in contrasting IAV and budget estimates when the spatio-temporal boundaries for the cross-comparison are too narrow (i.e., when comparing annual and stand-level estimates). Although it was beyond the scope of this study to address this challenge in more detail, our results emphasize the need to resolve the causes for the limited agreement on the IAV patterns of forest C budgets among various measurement approaches.

#### 4.2. Cross-scale assessments of drought impacts on the boreal forest C balance

Projections indicate that high-latitude regions will experience increases in temperature and changes in the water balance, which may cause more frequent and severe drought events during the 21st century (Gauthier et al., 2015; IPCC, 2021). Our ability for accurately quantifying and predicting the impacts of a changing climate and weather extremes on the C balance of boreal forests is therefore crucial for better understanding future forest C cycle-climate interactions (Gauthier et al., 2015; Lindroth et al., 2020; Martínez-García et al., 2024). Results from our cross-scale analysis suggest a good agreement of the NEP drought responses estimated with different measurement approaches at landscape and region scales. However, we noted a strong tendency towards greater drought sensitivity (i.e., greater reduction in NEP) in plot-scale

estimates based on forest-plot inventory and chamber-based flux measurements. This observation suggests that empirical assessments of the forest NEP response to drought may be scale- and/or method-dependent.

The greater drought sensitivity observed at the plot-scale may be due to fundamental differences in the temporal resolution and conceptual design of the forest-plot inventory and chamber-based approach compared to EC flux and atmospheric concentration measurements. Specifically, the NEP drought response estimated at the plot-scale primarily relies on the observed changes in annual stem diameter growth. This approach is based on two key assumptions: i) a direct relationship exists between stem diameter changes and ecosystem GPP, and ii) allometric relationships between stem diameter and tree biomass remain constant regardless of environmental conditions. However, both these assumptions may fail, particularly during drought (Cabon et al., 2022; Pretzsch et al., 2012; Rog et al., 2024). Another critical shortcoming in bottom-up approaches is the relatively infrequent sampling interval of manual chamber-based measurements, which may contribute to uncertainty in soil flux estimates by failing to accurately capture drought events. In contrast, EC measurements provide a direct estimate of the whole-ecosystem C cycle response to drought with high-temporal resolution (Lindroth et al., 2020), which is further valuable for developing process-based and data-driven models (Jung et al., 2020; Mo et al., 2008). Yet, the EC-based approach requires suitable terrain (flat, homogenous) and substantial resources and is therefore limited to relatively few measurement locations, making it less suitable for capturing variations in the NEP drought response across heterogeneous landscapes. We caution that the bias in our plot scale dataset towards smaller contribution from the younger age classes (Fig. 2b), which were found to be more sensitive to drought (Martínez-García et al., 2024), may have counterbalanced the observed scale divergence in the NEP drought response (i.e., implying an even greater divergence under more similar age class distribution). It is further noteworthy that in this study the landscape- and region-scale footprints of L-EC and ATM

measurements include contributions from non-forest ecosystems such as mires, agricultural lands, and inland waters. This may partly explain the divergent drought response when compared to plot- and ecosystem-/regional-scale estimates from the forested areas. Given these uncertainties in the light of ongoing climate change, advancing our understanding of cross-scale linkages between bottom-up and top-down estimates of the NEP drought response is a critical research frontier and prerequisite for improved predictions of forest C cycle-climate feedbacks.

#### 4.3. Spatially nested monitoring programs to constrain forest C cycle processes and budgets

The terrestrial biosphere-atmosphere exchange of C constitutes a highly non-linear and tightly coupled system, characterized by substantial variability across space and time (Desai et al., 2022b; Osmond et al., 2004). However, since our standard measurement approaches are inherently limited to distinct spatial and temporal scales, it remains key challenge to reconcile C cycle processes and their drivers across these scales (Bastviken et al., 2022; Desai et al., 2022b). Here, we demonstrate that nested measurement, integrating multiple spatial scales and multi-year observations, are essential for addressing this shortcoming.

Numerous studies have previously compared C balances across different spatial scales, however, they have typically focused on reconciling stand-level estimates derived from plot-scale and EC measurements (Campioli et al., 2016; Peichl et al., 2010) or on regional-scale estimates based on aircraft measurement and ATM approaches (Lauvaux et al., 2009), leaving a critical gap between local stand and regional scales. Our study advances this body of work by providing a 3-year measurement program along a plot- to region-scale continuum that fills this spatial gap with observations at the landscape scale. The spatial gap between plot/ecosystem-scale assessments and top-down estimates of regional budgets (i.e., hundred thousands of km<sup>2</sup>) is particularly critical in reaching agreement on the forest C balance for heterogeneous landscapes managed by rotation forestry (Kondo et al., 2020; Lauvaux et al., 2009; Sathyanadh et al., 2021). Here, pronounced gradients of stand age create a highly diversified mosaic of C dynamics that standard field measurement approaches commonly cannot adequately capture. At the same time, while top-down approaches and remote sensing products require ground-based data for validation, their estimates are rarely resolved at plot/ecosystem-scale resolution (Foster et al., 2023; Zhu et al., 2023). Recently, tall tower EC measurements have been proposed as a way forward to address this spatial disconnection by providing an interface between plot/ecosystem-scale and regional top-down approaches (Sathyanadh et al., 2021). Given a measurement footprint area with a radius of several kilometres (Chi et al., 2019; Kljun et al., 2015), tall tower EC measurements can bridge the critical spatial gap, thus allowing to link and reconcile C flux processes and budgets along a spatial continuum. Subsequently, these measurements can also provide a valuable observational basis for regional to global modelling approaches.

Although nested measurement frameworks, such as the one developed in this study, appear critical to advancing our understanding of the scale-dependence of the terrestrial C cycle, such extensive setups are currently scarce (Futter et al., 2023). A remarkable exception is the intensive campaign CHEESEHEAD19 (Butterworth et al., 2021), which integrated measurements from 19 EC towers, the central tall AmeriFlux tower US-PFa, ground-based measurement across 41 inventory plots, a suite of atmospheric profiling instruments, and airborne data collection over a 10 km × 10 km domain in a managed forest landscape in northern Wisconsin during four summer months in 2019. Previous research in this study area found that flux estimates from multiple ground-based EC towers were in relatively good agreement with those from the US-PFa tall tower after weighing the footprint contributions (Desai et al., 2008). In contrast, a more recent study concluded that upscaling of the results from the 19 flux towers in CHEESEHEAD19 initiative, as well as

long-term records from selected tower sites, agreed poorly with the integrated tall tower estimates, particularly in capturing IAV (Desai et al., 2022a). Such contrasting findings, even within the same measurement program, demonstrate the complexity of resolving the scale-dependency in C balance estimates for managed forest landscapes, and highlight the importance of cross-scale assessments. Although we acknowledge the limitation of resources for developing such extensive measurement setups, we suggest increasing the use of established infrastructure within the international networks of FLUXNET (global), ICOS (Europe), and NEON (USA) to deploy additional spatially-nested measurement programmes. This could be achieved by equipping atmospheric tall towers with EC instrumentation and/or establishing extensive grids of forest inventory-plots within the EC measurement footprints.

## 5. Conclusions

This study employed a spatially-nested measurement framework that integrates both bottom-up (forest-plot inventory and chamber-based fluxes) and top-down (eddy-covariance; atmospheric observations and atmospheric transport modelling) approaches to reconcile the C balance of actively managed boreal forests in Northern Sweden across plot-, ecosystem-, landscape-, and regional scales over three years (2016–2018). Based on our results, we conclude that estimates of the forest NEP and its components (i.e., GPP and Reco) derived across different spatial scales and using alternative approaches may reach reasonable agreement over multi-year timeframes and in the presence of cross-scale homogeneity in forest structure (e.g., stand age) and productivity. Specifically, we observed that the 3-year mean NEP converged into a C sink of  $118 \pm 27 \text{ g C m}^{-2} \text{ yr}^{-1}$  across plot-, landscape-, and regional scales. This underscores the significant C sink function of managed boreal forests and provides a valuable benchmark for evaluating alternative forest management strategies. However, our study also revealed notable inconsistencies among estimates of inter-annual variations in NEP, GPP and Reco across most spatial scales and approaches. These discrepancies are likely attributable to the different processes captured by each approach, reflecting the conceptual divergence in estimating C balances based on measurements of either fluxes (i.e., chamber- and EC-based methods), atmospheric concentrations (i.e., ATM), or ecosystem C stock changes (i.e., NFI). We further highlight the contrasting NEP responses to drought observed between bottom-up and top-down approaches. Overall, we conclude that the integration of multi-scale monitoring platforms, via co-locating bottom-up and top-down measurement approaches at existing tower stations, is a crucial step in advancing our understanding of how the boreal forest C cycle responds to anthropogenic pressures and interacts with the climate system across spatial and temporal scales.

### CRedit authorship contribution statement

**Matthias Peichl:** Writing – original draft, Supervision, Project administration, Methodology, Investigation, Funding acquisition, Formal analysis, Data curation, Conceptualization. **Eduardo Martínez-García:** Writing – review & editing, Visualization, Methodology, Investigation, Formal analysis, Data curation. **Jinshu Chi:** Writing – review & editing, Data curation. **Natascha Kljun:** Writing – review & editing, Methodology. **Anne Klosterhalfen:** Writing – review & editing, Data curation. **Johannes Larson:** Writing – review & editing, Data curation. **Hjalmar Laudon:** Writing – review & editing, Resources. **Tomas Lundmark:** Writing – review & editing, Resources. **Guillaume Monteil:** Writing – review & editing, Methodology, Data curation. **Mats B. Nilsson:** Writing – review & editing, Resources, Methodology. **Anusha Sathyanadh:** Writing – review & editing, Data curation. **Marko Scholze:** Writing – review & editing, Methodology. **Jörgen Wallerman:** Writing – review & editing, Data curation. **Peng Zhao:** Writing – review & editing, Data curation.

## Declaration of competing interest

The authors declare that they have no known competing financial interests or personal relationships that could have appeared to influence the work reported in this paper.

## Acknowledgements

This study was funded by the Swedish Research Council for Environment, Agricultural Sciences and Spatial Planning (FORMAS, grants 942-2015-49 and 2020-01446), the Kempe Foundations (grant SMK-1743 and JCK-1815) and the Knut and Alice Wallenberg Foundation (grants 2015.0047 and 2018.0259). Financial support from the Swedish Research Council and consortium partners provided to both the National Research Infrastructure ICOS Sweden (grants 2015-06020 and 2019-00205) and the Swedish Infrastructure for Ecosystem Science (SITES, grant 2017-00635) are acknowledged. We further acknowledge the data provided from the Swedish National Forest and Soil Inventories. Parts of the computations were enabled by resources provided by the National Academic Infrastructure for Supercomputing in Sweden (NAISS), partially funded by the Swedish Research Council (grant 2022-06725). The research presented in this paper is a contribution to the Strategic Research Areas 'Biodiversity and Ecosystem Services in a Changing Climate (BECC)' and 'Modelling the Regional and Global Earth system (MERGE)', both funded by the Swedish government. We thank the staff at the Unit for Field-based Forest Research, SLU, for support in field data collection.

## Supplementary materials

Supplementary material associated with this article can be found, in the online version, at [doi:10.1016/j.agrformet.2025.110926](https://doi.org/10.1016/j.agrformet.2025.110926).

## Data availability

The data supporting the findings of this study are openly available in the Zenodo digital repository at <https://doi.org/10.5281/zenodo.17581090>.

## References

- Ameray, A., Bergeron, Y., Valeria, O., Montoro Girona, M., Cavard, X., 2021. Forest Carbon Management: a review of silvicultural practices and management strategies across boreal, temperate and tropical forests. *Curr. For. Rep.* 7 (4), 245–266. <https://doi.org/10.1007/s40725-021-00151-w>.
- Anderson-Teixeira, K.J., Wang, M.M.H., McGarvey, J.C., Herrmann, V., Tepley, A.J., Bond-Lamberty, B., LeBauer, D.S., 2018. ForC: a global database of forest carbon stocks and fluxes. *Ecology* 99 (6). <https://doi.org/10.1002/ecy.2229>, 1507–1507.
- Artaxo, P., et al., 2022. Tropical and boreal Forest – Atmosphere interactions: a review. *Tellus B: Chem. Phys. Meteorol.* 74 (2022), 2022. <https://doi.org/10.16993/tellusb.34>. Article.
- Astrup, R., Bernier, P.Y., Genet, H., Lutz, D.A., Bright, R.M., 2018. A sensible climate solution for the boreal forest. *Nat. Clim. Chang.* 8 (1), 11–12. <https://doi.org/10.1038/s41558-017-0043-3>.
- Baldocchi, D., Chu, H., Reichstein, M., 2018. Inter-annual variability of net and gross ecosystem carbon fluxes: a review. *Agric. For. Meteorol.* 249, 520–533. <https://doi.org/10.1016/j.agrformet.2017.05.015>.
- Bastviken, D., Wilk, J., Duc, N.T., Gålfalk, M., Karlson, M., Neset, T.-S., Opach, T., Enrich-Prast, A., Sundgren, I., 2022. Critical method needs in measuring greenhouse gas fluxes. *Environ. Res. Lett.* 17 (10), 104009. <https://doi.org/10.1088/1748-9326/ac8fa9>.
- Bellassen, V., Luysaert, S., 2014. Carbon sequestration: managing forests in uncertain times. *Nature* 506 (7487), 153–155. <https://doi.org/10.1038/506153a>.
- Bradshaw, C.J.A., Warkentin, I.G., 2015. Global estimates of boreal forest carbon stocks and flux. *Glob. Planet. Change* 128, 24–30. <https://doi.org/10.1016/j.gloplacha.2015.02.004>.
- Butterworth, B.J., et al., 2021. Connecting land–Atmosphere interactions to surface heterogeneity in CHEESEHEAD19. *Bull. Am. Meteorol. Soc.* 102 (2), E421–E445. <https://doi.org/10.1175/BAMS-D-19-0346.1>.
- Cabon, A., et al., 2022. Cross-biome synthesis of source versus sink limits to tree growth. *Science* (1979) 376 (6594), 758–761. <https://doi.org/10.1126/science.abm4875>.
- Campoli, M., Malhi, Y., Vicca, S., Luysaert, S., Papale, D., Peñuelas, J., Reichstein, M., Migliavacca, M., Arain, M.A., Janssens, I.A., 2016. Evaluating the convergence between eddy-covariance and biometric methods for assessing carbon budgets of forests. *Nat. Commun.* 7 (1). <https://doi.org/10.1038/ncomms13717>.
- Carvalho, N., Forkel, M., Khomik, M., Bellarby, J., Jung, M., Migliavacca, M., Reichstein, M., 2014. Global covariation of carbon turnover times with climate in terrestrial ecosystems. *Nature* 514 (7521), 213–217. <https://doi.org/10.1038/nature13731>.
- Chi, J., Nilsson, M.B., Kljun, N., Wallerman, J., Fransson, J.E.S., Laudon, H., Lundmark, T., Peichl, M., 2019. The carbon balance of a managed boreal landscape measured from a tall tower in northern Sweden. *Agric. For. Meteorol.* 274, 29–41. <https://doi.org/10.1016/j.agrformet.2019.04.010>.
- Chi, J., Nilsson, M.B., Laudon, H., Lindroth, A., Wallerman, J., Fransson, J.E.S., Kljun, N., Lundmark, T., Löfvenius, M.O., Peichl, M., 2020. The Net landscape carbon balance—Integrating terrestrial and aquatic carbon fluxes in a managed boreal forest landscape in Sweden. *Glob. Chang. Biol.* 26 (4), 2353–2367. <https://doi.org/10.1111/gcb.14983>.
- Chi, J., Zhao, P., Klosterhalfen, A., Joher, G., Kljun, N., Nilsson, M.B., Peichl, M., 2021. Forest floor fluxes drive differences in the carbon balance of contrasting boreal forest stands. *Agric. For. Meteorol.* 306, 108454. <https://doi.org/10.1016/j.agrformet.2021.108454>.
- Desai, A.R., Helliiker, B.R., Moorcroft, P.R., Andrews, A.E., Berry, J.A., 2010. Climatic controls of interannual variability in regional carbon fluxes from top-down and bottom-up perspectives. *J. Geophys. Res.: Biogeosci.* 115 (G2). <https://doi.org/10.1029/2009JG001122>.
- Desai, A.R., Murphy, B.A., Wiesner, S., Thom, J., Butterworth, B.J., Koupaei-Abyazani, N., Muttaqin, A., Paleri, S., Talib, A., Turner, J., Mineau, J., Merrelli, A., Stoy, P., Davis, K., 2022a. Drivers of decadal carbon fluxes across temperate ecosystems. *J. Geophys. Res.: Biogeosci.* 127 (12), e2022JG007014. <https://doi.org/10.1029/2022JG007014>.
- Desai, A.R., Noormets, A., Bolstad, P.V., Chen, J., Cook, B.D., Davis, K.J., Euskirchen, E.S., Gough, C., Martin, J.G., Ricciuto, D.M., Schmid, H.P., Tang, J., Wang, W., 2008. Influence of vegetation and seasonal forcing on carbon dioxide fluxes across the Upper Midwest, USA: implications for regional scaling. *Agric. For. Meteorol.* 148 (2), 288–308. <https://doi.org/10.1016/j.agrformet.2007.08.001>.
- Desai, A.R., Paleri, S., Mineau, J., Kadum, H., Wanner, L., Mauder, M., Butterworth, B.J., Durden, D.J., Metzger, S., 2022b. Scaling land-atmosphere interactions: special or fundamental? *J. Geophys. Res.: Biogeosci.* 127 (10), e2022JG007097. <https://doi.org/10.1029/2022JG007097>.
- European Commission, 2021. Fit for 55°. Delivering the EU's 2030 Climate Target On the Way to Climate neutrality, 14. European Commission, Brussels.
- Foster, K.T., Sun, W., Shiga, Y.P., Mao, J., Michalak, A.M., 2023. Multiscale assessment of North American terrestrial carbon balance. *Biogeosci. Discuss.* 1–31. <https://doi.org/10.5194/bg-2023-111>.
- Franz, D., et al., 2018. Towards long-term standardised carbon and greenhouse gas observations for monitoring Europe's terrestrial ecosystems: a review. *Int. Agrophys.* 32 (4), 439–455. <https://doi.org/10.1515/intag-2017-0039>.
- Fridman, J., Holm, S., Nilsson, M., Nilsson, P., Ringvall, A.H., Ståhl, G., 2014. Adapting National Forest Inventories to changing requirements – the case of the Swedish National Forest Inventory at the turn of the 20th century. *Silva Fennica* 48 (3). <https://www.silvafennica.fi/article/1095>.
- Futter, M.N., Dirnböck, T., Forsius, M., Bäck, J.K., Cools, N., Diaz-Pines, E., Dick, J., Gaube, V., Gillespie, L.M., Högbom, L., Laudon, H., Mirtl, M., Nikolaidis, N., Poppe Terán, C., Skiba, U., Vereecken, H., Villwock, H., Weldon, J., Wohner, C., Alam, S.A., 2023. Leveraging research infrastructure co-location to evaluate constraints on terrestrial carbon cycling in northern European forests. *Ambio* 52 (11), 1819–1831. <https://doi.org/10.1007/s13280-023-01930-4>.
- Gauthier, S., Bernier, P., Kuuluvainen, T., Shvidenko, A.Z., Schepaschenko, D.G., 2015. Boreal forest health and global change. *Science* (1979) 349, 819–822. <https://doi.org/10.1126/science.aaa9092>.
- Giles-Hansen, K., Wei, X., 2022. Cumulative disturbance converts regional forests into a substantial carbon source. *Environ. Res. Lett.* 17 (4), 044049. <https://doi.org/10.1088/1748-9326/ac5e69>.
- Hadden, D., Grelle, A., 2016. Changing temperature response of respiration turns boreal forest from carbon sink into carbon source. *Agric. For. Meteorol.* 223, 30–38. <https://doi.org/10.1016/j.agrformet.2016.03.020>.
- Hadden, D., Grelle, A., 2017. Net CO<sub>2</sub> emissions from a primary boreo-nemoral forest over a 10-year period. *For. Ecol. Manage.* 398, 164–173. <https://doi.org/10.1016/j.foreco.2017.05.008>.
- Högberg, P., Arnesson Ceder, L., Astrup, R., Binkley, D., Bright, R., Dalsgaard, L., Egnell, G., Filipchuk, A., Genet, H., Ilintsev, A., Kurz, W.A., Laganière, J., Lemprière, T., Lundblad, M., Lundmark, T., Mäkipää, R., Malysheva, N., Mohr, C.W., Nordin, A., ... & Kraxner, F. ((2021) Sustainable boreal forest management - challenges and opportunities for climate change mitigation. Report from an insight process conducted by a team appointed by the International Boreal Forest Research Association (IBFRA). Swedish Forest Agency Report No. 11.
- Hyrynen, M., Ollikainen, M., Seppälä, J., 2023. European forest sinks and climate targets: past trends, main drivers, and future forecasts. *Eur. J. For. Res.* 142 (5), 1207–1224. <https://doi.org/10.1007/s10342-023-01587-4>.
- IPCC, 2021. Climate Change 2021: the physical science basis. In: Masson-Delmotte, V., Zhai, P., Pirani, A., Connors, S.L., Péan, C., Berger, S., Caud, N., Chen, Y., Goldfarb, L., Gomis, M.I., Huang, M., Leitzell, K., Lonnoy, E., Matthews, J.B.R., Maycock, T.K., Waterfield, T., Yelekçi, O., Yu, R., Zhou, B. (Eds.), Contribution of Working Group I to the Sixth Assessment Report of the Intergovernmental Panel On Climate Change. Cambridge University Press, Cambridge, United Kingdom and New York, NY, USA, p. 2391.

- Jung, M., et al., 2020. Scaling carbon fluxes from eddy covariance sites to globe: synthesis and evaluation of the FLUXCOM approach. *Biogeosciences* 17 (5), 1343–1365. <https://doi.org/10.5194/bg-17-1343-2020>.
- Keenan, T., et al., 2012. Terrestrial biosphere model performance for inter-annual variability of land-atmosphere CO<sub>2</sub> exchange. *Glob. Chang. Biol.* 18 (6), 1971–1987. <https://doi.org/10.1111/j.1365-2486.2012.02678.x>.
- Kljun, N., Black, T.A., Griffis, T.J., Barr, A.G., Gaumont-Guay, D., Morgenstern, K., McCaughey, J.H., Nescic, Z., 2006. Response of net ecosystem productivity of three boreal forest stands to drought. *Ecosystems* 9 (7), 1128–1144. <https://doi.org/10.1007/s10021-005-0082-x>.
- Kljun, N., Calanca, P., Rotach, M.W., Schmid, H.P., 2015. A simple two-dimensional parameterisation for flux footprint prediction (FFP). *Geosci. Model. Dev.* 8 (11), 3695–3713. <https://doi.org/10.5194/gmd-8-3695-2015>.
- Klosterhalfen, A., Chi, J., Kljun, N., Lindroth, A., Laudon, H., Nilsson, M.B., Peichl, M., 2023. Two-level eddy covariance measurements reduce bias in land-atmosphere exchange estimates over a heterogeneous boreal forest landscape. *Agric. For. Meteorol.* 339, 109523. <https://doi.org/10.1016/j.agrformet.2023.109523>.
- Kondo, M., et al., 2020. State of the science in reconciling top-down and bottom-up approaches for terrestrial CO<sub>2</sub> budget. *Glob. Chang. Biol.* 26 (3), 1068–1084. <https://doi.org/10.1111/gcb.14917>.
- Krinner, G., Viovy, N., de Noblet-Ducoudré, N., Ogée, J., Polcher, J., Friedlingstein, P., Ciais, P., Sitch, S., Prentice, I.C., 2005. A dynamic global vegetation model for studies of the coupled atmosphere-biosphere system. *Glob. Biogeochem. Cycle* 19 (1). <https://doi.org/10.1029/2003GB002199>.
- Laudon, H., Hasselquist, E.M., Peichl, M., Lindgren, K., Sponseller, R., Lidman, F., Kuglerová, L., Hasselquist, N.J., Bishop, K., Nilsson, M.B., Ågren, A.M., 2021. Northern landscapes in transition: evidence, approach and ways forward using the Krycklan Catchment Study. *Hydro. Process.* 35 (4), e14170. <https://doi.org/10.1002/hyp.14170>.
- Lauvaux, T., Gioli, B., Sarraz, C., Rayner, P.J., Ciais, P., Chevallier, F., Noilhan, J., Miglietta, F., Brunet, Y., Ceschia, E., Dolman, H., Elbers, J.A., Gerbig, C., Hutjes, R., Jarosz, N., Legain, D., Uliasz, M., 2009. Bridging the gap between atmospheric concentrations and local ecosystem measurements. *Geophys. Res. Lett.* 36 (19), L19809. <https://doi.org/10.1029/2009GL039574>.
- Lemprière, T.C., Kurz, W.A., Hogg, E.H., Schmoll, C., Rampley, G.J., Yemshanov, D., McKenney, D.W., Gilsenan, R.P., Beatch, A., Blain, D., Bhatti, J.S., & Krmar, E. (2013). *Canadian boreal forests and climate change mitigation*. 21(4), 293–321. [10.1139/er-2013-0039](https://doi.org/10.1139/er-2013-0039).
- Lindroth, A., Holst, J., Linderson, M.-L., Aurela, M., Biermann, T., Heliasz, M., Chi, J., Ibram, A., Kolari, P., Klemetsson, L., Krasnova, A., Laurila, T., Lehner, I., Lohila, A., Mammarella, I., Mölder, M., Löfvenius, M.O., Peichl, M., Pilegaard, K., Nilsson, M., 2020. Effects of drought and meteorological forcing on carbon and water fluxes in Nordic forests during the dry summer of 2018. *Philosoph. Transact. Roy. Soc. B: Biol. Sci.* 375 (1810), 20190516. <https://doi.org/10.1098/rstb.2019.0516>.
- Lundmark, T., Bergh, J., Hofer, P., Lundström, A., Nordin, A., Poudel, B.C., Sathre, R., Taverna, R., Werner, F., 2014. Potential roles of Swedish forestry in the context of climate change mitigation. *Forests* 5 (4), 557–578. <https://doi.org/10.3390/f5040557>.
- Luyssaert, S., Inglima, I., Jung, M., Richardson, a.D., Reichstein, M., Papale, D., Piao, S. L., Schulze, E.-d., Wingate, L., Matteucci, G., Aragao, L., Aubinet, M., Beer, C., Bernhofer, C., Black, K.G., Bonal, D., Bonnefond, J.-m., Chambers, J., Ciais, P., Janssens, I.A., 2007. CO<sub>2</sub> balance of boreal, temperate, and tropical forests derived from a global database. *Glob. Chang. Biol.* 13 (12), 2509–2537. <https://doi.org/10.1111/j.1365-2486.2007.01439.x>.
- Mahadevan, P., Wofsy, S.C., Matross, D.M., Xiao, X., Dunn, A.L., Lin, J.C., Gerbig, C., Munger, J.W., Chow, V.Y., Gottlieb, E.W., 2008. A satellite-based biosphere parameterization for net ecosystem CO<sub>2</sub> exchange: vegetation photosynthesis and respiration model (VPRM). *Glob. Biogeochem. Cycle* 22 (2). <https://doi.org/10.1029/2006GB002735>.
- Marklund, L.G., 1988. *Biomass Functions pine, Spruce and Birch in Sweden. Department of Forest Survey, Swedish University of Agricultural Sciences, Uppsala, Sweden.*
- Martínez-García, E., Nilsson, M.B., Laudon, H., Lundmark, T., Fransson, J.E.S., Wallerman, J., Peichl, M., 2022. Overstory dynamics regulate the spatial variability in forest-floor CO<sub>2</sub> fluxes across a managed boreal forest landscape. *Agric. For. Meteorol.* 318, 108916. <https://doi.org/10.1016/j.agrformet.2022.108916>.
- Martínez-García, E., Nilsson, M.B., Laudon, H., Lundmark, T., Fransson, J.E.S., Wallerman, J., Peichl, M., 2024. Drought response of the boreal forest carbon sink is driven by understorey–tree composition. *Nat. Geosci.* 17 (3), 197–204. <https://doi.org/10.1038/s41561-024-01374-9>.
- Mo, X., Chen, J.M., Ju, W., Black, T.A., 2008. Optimization of ecosystem model parameters through assimilating eddy covariance flux data with an ensemble Kalman filter. *Ecol. Modell.* 217 (1), 157–173. <https://doi.org/10.1016/j.ecolmodel.2008.06.021>.
- Montei, G., Scholze, M., 2021. Regional CO<sub>2</sub> inversions with LUMIA, the Lund University Modular Inversion Algorithm, v1.0. *Geosci. Model. Dev.* 14 (6), 3383–3406. <https://doi.org/10.5194/gmd-14-3383-2021>.
- Osmond, B., Ananyev, G., Berry, J., Langdon, C., Kolber, Z., Lin, G., Monson, R., Nichol, C., Rascher, U., Schurr, U., Smith, S., Yakir, D., 2004. Changing the way we think about global change research: scaling up in experimental ecosystem science. *Glob. Chang. Biol.* 10 (4), 393–407. <https://doi.org/10.1111/j.1529-8817.2003.00747.x>.
- O’Sullivan, M., Sitch, S., Friedlingstein, P., Luijckx, I.T., Peters, W., Rosan, T.M., Arnett, A., Arora, V.K., Chandra, N., Chevallier, F., Ciais, P., Falk, S., Feng, L., Gasser, T., Houghton, R.A., Jain, A.K., Kato, E., Kennedy, D., Knauer, J., Zaehle, S., 2024. The key role of forest disturbance in reconciling estimates of the northern carbon sink. *Commun. Earth. Environ.* 5 (1), 1–10. <https://doi.org/10.1038/s43247-024-01827-4>.
- Pan, Y., Birdsey, R.A., Fang, J., Houghton, R., Kauppi, P.E., Kurz, W.A., Phillips, O.L., Shvidenko, A., Lewis, S.L., Canadell, J.G., Ciais, P., Jackson, R.B., Pacala, S.W., McGuire, A.D., Piao, S., Rautiainen, A., Sitch, S., Hayes, D., 2011. A large and persistent carbon sink in the world’s forests. *Science* (1979) 333 (6045), 988–993. <https://doi.org/10.1126/science.1201609>.
- Pan, Y., Birdsey, R.A., Phillips, O.L., Houghton, R.A., Fang, J., Kauppi, P.E., Keith, H., Kurz, W.A., Ito, A., Lewis, S.L., Nabuurs, G.-J., Shvidenko, A., Hashimoto, S., Lerink, B., Schepaschenko, D., Castanho, A., Murdiyarso, D., 2024. The enduring world forest carbon sink. *Nature* 631 (8021), 563–569. <https://doi.org/10.1038/s41586-024-07602-x>.
- Peichl, M., Brodeur, J.J., Khomik, M., Arain, M.A., 2010. Biometric and eddy-covariance based estimates of carbon fluxes in an age-sequence of temperate pine forests. *Agric. For. Meteorol.* 150 (7–8), 952–965. <https://doi.org/10.1016/j.agrformet.2010.03.002>.
- Peichl, M., Martínez-García, E., Fransson, J.E.S., Wallerman, J., Laudon, H., Lundmark, T., Nilsson, M.B., 2023a. Landscape-variability of the carbon balance across managed boreal forests. *Glob. Chang. Biol.* 29 (4), 1119–1132. <https://doi.org/10.1111/gcb.16534>.
- Peichl, M., Martínez-García, E., Fransson, J.E.S., Wallerman, J., Laudon, H., Lundmark, T., Nilsson, M.B., 2023b. On the uncertainty in estimates of the carbon balance recovery time after forest clear-cutting. *Glob. Chang. Biol.* 29 (15), e1–e3. <https://doi.org/10.1111/gcb.16772>.
- Peters, W., Bastos, A., Ciais, P., Vermeulen, A., 2020. A historical, geographical and ecological perspective on the 2018 European summer drought. *Philos. Trans. R. Soc. Lond., B, Biol. Sci.* 375 (1810), 20190505. <https://doi.org/10.1098/rstb.2019.0505>.
- Pettersson, H., Ellison, D., Appiah Mensah, A., Berndes, G., Egnell, G., Lundblad, M., Lundmark, T., Lundström, A., Stendahl, J., Wikberg, P.-E., 2022. On the role of forests and the forest sector for climate change mitigation in Sweden. *GCB Bioenergy* 14 (7), 793–813. <https://doi.org/10.1111/gcbb.12943>.
- Pettersson, H., Ståhl, G., 2006. Functions for below-ground biomass of *Pinus sylvestris*, *Picea abies*, *Betula pendula* and *Betula pubescens* in Sweden. *Scandinav. J. Forest Res.* 21 (S7), 84–93. <https://doi.org/10.1080/14004080500486864>.
- Piao, S., et al., 2013. Evaluation of terrestrial carbon cycle models for their response to climate variability and to CO<sub>2</sub> trends. *Glob. Chang. Biol.* 19 (7), 2117–2132. <https://doi.org/10.1111/gcb.12187>.
- Pisso, I., Sollum, E., Grythe, H., Kristiansen, N.I., Cassiani, M., Eckhardt, S., Arnold, D., Morton, D., Thompson, R.L., Groot Zwaafink, C.D., Evangeliou, N., Sodemann, H., Haimberger, L., Henne, S., Brunner, D., Burkhardt, J.F., Fouilloux, A., Brioude, J., Philipp, A., Stohl, A., 2019. The lagrangian particle dispersion model FLEXPART version 10.4. *Geosci. Model. Dev.* 12 (12), 4955–4997. <https://doi.org/10.5194/gmd-12-4955-2019>.
- Pretzsch, H., Uhl, E., Biber, P., Schütze, G., Coates, K.D., 2012. Change of allometry between coarse root and shoot of Lodgepole pine (*Pinus contorta* DOUGL. ex LOUD) along a stress gradient in the sub-boreal forest zone of British Columbia. *Scandinav. J. Forest Res.* 27 (6), 532–544. <https://doi.org/10.1080/02827581.2012.672583>.
- Reichstein, M., et al., 2005. On the separation of net ecosystem exchange into assimilation and ecosystem respiration: review and improved algorithm. *Glob. Chang. Biol.* 11 (9), 1424–1439. <https://doi.org/10.1111/j.1365-2486.2005.001002.x>.
- Repola, J., 2008. Biomass equations for birch in Finland. *Silva Fennica* 42 (4). <https://doi.org/10.14214/sf.236>.
- Roebrock, C.T.J., Duveiller, G., Seneviratne, S.I., Davin, E.L., Cescatti, A., 2023. Releasing global forests from human management: how much more carbon could be stored? *Science* (1979) 380 (6646), 749–753. <https://doi.org/10.1126/science.add5878>.
- Rog, I., Hilman, B., Fox, H., Yalin, D., Qubaja, R., Klein, T., 2024. Increased belowground tree carbon allocation in a mature mixed forest in a dry versus a wet year. *Glob. Chang. Biol.* 30 (2), e17172. <https://doi.org/10.1111/gcb.17172>.
- Sathyanadh, A., Monteil, G., Scholze, M., Klosterhalfen, A., Laudon, H., Wu, Z., Gerbig, C., Peters, W., Bastrikov, V., Nilsson, M.B., Peichl, M., 2021. Reconciling the carbon balance of Northern Sweden through integration of observations and modelling. *J. Geophys. Res.: Atmosph.* 126 (23), e2021JD035185. <https://doi.org/10.1029/2021JD035185>.
- Shorohova, E., Kapitsa, E., Vanha-Majamaa, I., 2008. Decomposition of stumps 10 years after partial and complete harvesting in a southern boreal forest in Finland. *Canad. J. Forest Res.* 38 (9), 2414–2421. <https://doi.org/10.1139/X08-083>.
- Sippel, S., Reichstein, M., Ma, X., Mahecha, M.D., Lange, H., Flach, M., Frank, D., 2018. Drought, heat, and the carbon cycle: a review. *Curr. Clim. Change Rep.* 4 (3), 266–286. <https://doi.org/10.1007/s40641-018-0103-4>.
- Smith, B., Wärlind, D., Arnett, A., Hickler, T., Leadley, P., Siltberg, J., Zaehle, S., 2014. Implications of incorporating N cycling and N limitations on primary production in an individual-based dynamic vegetation model. *Biogeosciences* 11 (7), 2027–2054. <https://doi.org/10.5194/bg-11-2027-2014>.
- Tang, J., Luyssaert, S., Richardson, A.D., Kutsch, W., Janssens, I.A., 2014. Steeper declines in forest photosynthesis than respiration explain age-driven decreases in forest growth. *Proceed. Natl. Acad. Sci.* 111 (24), 8856–8860. <https://doi.org/10.1073/pnas.1320761111>.
- UNFCCC. (2023a). National inventory Document Sweden 2025: greenhouse gas emission inventories 1990–2023. United Nations Framework Convention on Climate Change. <https://unfccc.int/documents/646476>.
- UNFCCC. (2023b). Common Reporting Table Sweden 2025: greenhouse gas emission inventories 1990–2023. United Nations Framework Convention on Climate Change. <https://unfccc.int/documents/646478>.

- Virkkala, A.-M., et al., 2025. Wildfires offset the increasing but spatially heterogeneous Arctic–boreal CO<sub>2</sub> uptake. *Nat. Clim. Chang.* 15 (2), 188–195. <https://doi.org/10.1038/s41558-024-02234-5>.
- Yatskov, M., Harmon, M.E., Krankina, O.N., 2003. A chronosequence of wood decomposition in the boreal forests of Russia. *Canad. J. Forest Res.* 33 (7), 1211–1226. <https://doi.org/10.1139/x03-033>.
- Zeng, J., Matsunaga, T., Tan, Z.-H., Saigusa, N., Shirai, T., Tang, Y., Peng, S., Fukuda, Y., 2020. Global terrestrial carbon fluxes of 1999–2019 estimated by upscaling eddy covariance data with a random forest. *Sci. Data* 7 (1), 313. <https://doi.org/10.1038/s41597-020-00653-5>.
- Zhao, P., Chi, J., Nilsson, M.B., Löfvenius, M.O., Högberg, P., Jocher, G., Lim, H., Mäkelä, A., Marshall, J., Ratcliffe, J., Tian, X., Näsholm, T., Lundmark, T., Linder, S., Peichl, M., 2022. Long-term nitrogen addition raises the annual carbon sink of a boreal forest to a new steady-state. *Agric. For. Meteorol.* 324, 109112. <https://doi.org/10.1016/j.agrformet.2022.109112>.
- Zhu, S., Olde, L., Lewis, K., Quaife, T., Cardenas, L., Loick, N., Xu, J., Hill, T., 2023. Eddy covariance fluxes over managed ecosystems extrapolated to field scales at fine spatial resolutions. *Agric. For. Meteorol.* 342, 109675. <https://doi.org/10.1016/j.agrformet.2023.109675>.